Hindawi
Advances in Materials Science and Engineering
Volume 2020, Article ID 6635507, 13 pages
https://doi.org/10.1155/2020/6635507

Research Article

Enhanced Mechanical Properties of Mg-6Sn-3Al-1Zn Alloy with Bimodal Grain Size Disturbed in the Microstructure Uniformly through Changing the Rolling Temperature

Fuan Wei,[1] Jinhui Wang,[1] Ping Li,[2] and Bo Shi[1]

[1]*Qinghai Provincial Key Laboratory of New Light Alloys, Qinghai Provincial Engineering Research Center of High Performance Light Metal Alloys and Forming, Qinghai University, Xining 810016, China*
[2]*College of Eco-Environmental Engineering, Qinghai University, Xining 810016, China*

Correspondence should be addressed to Bo Shi; boshi@qhu.edu.cn

Received 7 October 2020; Revised 17 November 2020; Accepted 23 November 2020; Published 24 December 2020

Academic Editor: Jinyang Xu

The mechanical properties of Mg-6Sn-3Al-1Zn alloy were enhanced with bimodal grain size disturbed in the microstructure uniformly; the Mg-6Sn-3Al-1Zn alloys were rolled with 60% thickness reduction at different rolling temperatures. The results have shown that the Mg-6Sn-3Al-1Zn alloys are composed of Mg_2Sn phase and α-Mg matrix phase. When the rolling temperature was less than or equal to 400°C, with the rolling temperature increasing, the average size and volume fraction of Mg_2Sn phase and the average grain size of small grains remained unchanged, the average grain size of large grains decreased, the volume fraction of small grains increased, and the yield strength of the alloy increased. When the rolling temperature reached 450°C, the average size and volume fraction of Mg_2Sn phase and the average grain size of large grains increased, and the volume fraction of small grains and the yield strength of the alloy decreased. The elongation increased with the rolling temperature increasing, but the change trend of hardness was just opposite. When the alloy was rolled at 400°C, the average sizes of small grains, large grains, and Mg_2Sn phases were 3.66 μm, 9.24 μm, and 19.5 μm, respectively. The volume fractions of small grains, large grains, and Mg_2Sn phases were 18.6%, 77.6%, and 3.8%, respectively. And the tensile properties reached the optimum; for example, the tensile strength, yield strength, elongation, and Vickers hardness were 361 MPa, 289.5 MPa, 20.5%, and 76.3 HV, respectively.

1. Introduction

Magnesium alloys are the lightest metallic structural materials [1–3]. Besides, magnesium alloys have widespread applications in modern aerospace, automobile industries, and electrical appliances, due to their strong specific strength, excellent electrode conductivity, electromagnetic shielding capability, and being easy to reuse [4–8]. In other words, magnesium alloys play an important role in modern industry.

Both the strength and ductility of the alloy cannot be enhanced at the same time. How to improve the strength and ductility of the alloy is a hot research topic. The research has found that bimodal microstructures formed in magnesium alloys or Al–Mg alloys could simultaneously improve the strength and ductility [9–13].

In recent years, many researchers have executed a mass of works on the study of rolling magnesium alloys, and they have developed many technologies to obtain high mechanical properties magnesium alloy sheets [14–16]. However, the effect of rolling temperature on the microstructure and mechanical properties of Mg-6Sn-3Al-1Zn alloy was seldom studied systematically. Due to being without rare earth elements, Mg-6Sn-3Al-1Zn alloys have low cost. In this paper, the optimum rolling temperature was found out, and the evolution of microstructure and mechanical properties was systematically investigated. Bimodal microstructure of Mg-6Sn-3Al-1Zn alloy was obtained when the rolling temperature was more than or equal to 350°C (the amount of rolling deformation was fixed at 60%). After the Mg-6Sn-3Al-1Zn alloy was rolled at 400°C, large grains and

small grains of bimodal microstructure distributed uniformly in the alloy, which leads to simultaneous enhancements of the strength and ductility of Mg-6Sn-3Al-1Zn alloy compared to the casting alloy. The present studies have significant value for the development of high mechanical properties Mg-6Sn-3Al-1Zn alloy, and the guiding function for fabricating high mechanical properties magnesium alloys in the future.

2. Experimental

2.1. Fabrication of Mg-6Sn-3Al-Zn Alloy. Firstly, the Mg, Sn, Al, and Zn bulks were weighted according to the weight ratio of Mg-6Sn-3Al-Zn alloy. Subsequently, Mg, Al, Zn bulks, refining agent, and molds were put into the resistance furnace for heat preservation at 300°C for 12 h. Due to the low melting point of Sn, then Sn bulk was dried by a dryer. The preheated Mg bulk was put into the smelting furnace and the mix gas (the volume ratio of Ar and SF_6 was 1 : 99) was introduced. After setting the temperature of the furnace as 800°C, Mg bulks were heated. When the Mg bulks were melted, the Sn, Zn, and Al bulks were added in order. When the melt temperature reached 730°C, 36 g refining agent was added and then fully agitated and the impurities were removed. The melt temperature was constantly heated to 750°C and kept for 20 min, and then the power supply was shut down for cooling the melt. When the temperature of the melt gradually reduced to 730°C, it was cast in a mold which was preheated to 300°C. After the melt solidification, the Mg-6Sn-3Al-Zn alloy was taken out from the mold.

2.2. Preparation of the As-Rolled Mg-3Al-6Sn-1Zn Alloy Samples. The cylindrical magnesium alloy was milled to a cuboid form using a milling machine. And the sample was solution-treated at 450°C for 8 h and then was water-quenched. The cubic sample was processed by wire cutting to obtain the magnesium alloy sheets (30 mm (width) × 50 mm (length) × 5 mm (thickness)). We fixed the amount of rolling deformation at 60% and selected 300°C, 350°C, 400°C, and 450°C as the rolling temperature. Before rolling, the mill roller was heated to 200°C, and the sample was held for 15 min at rolling temperature. The rolling reduction of the first rolling pass was 1 mm, and the subsequent rolling reduction was 0.3 mm, and the sample was kept warm in a resistance furnace with 2 min between the two passes.

2.3. Microstructure Characterization and Mechanical Properties Test. Firstly, the rolling samples were cut to be sheet samples (12 mm (length) × 6 mm (width)) along the rolling direction. Subsequently, these sheet samples were strictly disposed by the abrasive papers and mechanical polisher. These polishing slices were immediately etched for 25 s using the etch liquid (CH_3CH_2OH including 4% HNO_3). Finally, we observed the microstructure of the samples by using metallographic microscope (OM, DMI3000, Leica, Weztlar, Germany). The phases of magnesium alloy were identified by x-ray diffraction (XRD, BRUKERXD8ADVANCE-A25, Bruker, Karlsruhe, Germany) with a scan range of 20°–90°, a scan step of 0.02°. And the microstructure was observed using scanning electron microscopy (SEM, Merlin Campact, Carl Zeiss Microscopy Ltd., Jena, Germany) with an acceleration voltage of 20 kV and an electric current of 10 μA.

The grain size was characterized by Electron Back-Scattered Diffraction (EBSD, Oxford Instruments, Oxford, UK). We cut 5 mm (length) × 3 mm (width) in the center of the sample along the rolling direction, annealed it at 350°C for 5 min to remove stress, and polished it with 400#, 800#, 1200#, 2000#, 3000#, 5000#, and 7000# sandpapers, respectively. And then the samples were electrochemically polished with 7% perchlorate alcohol solution. Before electrochemical polishing, liquid nitrogen was added to the electrolyte solution to ensure the temperature of the electrolyte solution of -25°C. Polishing voltage, current, and time were 20 V, 0.2 μA, and 2 min, respectively. Argon ion polishing was carried out after electropolishing, polished voltage was 3 keV, polished angle was 3°, polished time was 90 min, and then the sample was observed by SEM equipped with EBSD from Oxford instrument, operating voltage and step were 20 kV and 0.21 μm, respectively, and EBSD patterns were indexed by using CHANNEL 5 software from HKL Technology, Oxford Instruments.

The dislocation analysis was characterized by transmission electron microscope (TEM, JEM-2010 HR, JEOL Ltd., Tokyo, Japan). Firstly, we used a wire cutting machine to cut a sample of 20 mm (length) × 20 mm (width). Secondly, the sample was thinned by sandpaper until its thickness decreased to 40 μm. Thirdly, TEM specimens were prepared by polishing machine (Model 110 Automatic Twin-Jet Electropolisher, E.A. Fischione Instruments, USA) used with an electrolyte solution composed of 4 vol% of $HClO_4$ and 96 vol % of C_2H_5OH. Fourthly, the sample was further reduced by a precision ion polishing system (PIPS, Gatan II 695, Pleasanton, USA). Lastly, the sample was observed by TEM at an operating voltage of 200 kV and a current of 103 μA.

The sheet samples were measured under 0.2 kgf loading force and dwelling 10 s using Vickers hardness tester (WILSON VH1102 type, Buehler, Illinois Tool Works Inc., Lake Bluff, USA). After 5-time measurements, we acquired the average value of Vickers hardness as the final value. Tensile properties were tested on an electronic universal testing machine (AGS-X-50 kN, Shimadzu, Tokyo, Japan) with a cross-head speed of 0.2 mm/min and repeated three times; the average value was as the final value.

3. Results

The XRD patterns of Mg-6Sn-3Al-Zn alloys without and with rolling at different temperatures are shown in Figure 1. As can be seen, the phases include α-Mg matrix and Mg_2Sn second phase, indicating that the phase compositions are steady at various rolling temperatures. The (0002) diffraction peak intensity increased after rolling, while the (10-10) and (10-11) diffraction peak intensity decreased. This indicates that the (0002) basal texture was formed in Mg-6Sn-3Al-Zn alloy after rolling at different temperatures.

Basal plane (0002), prismatic plane (10-10), and (11-20) pole figures of Mg-6Sn-3Al-Zn alloys rolled at different

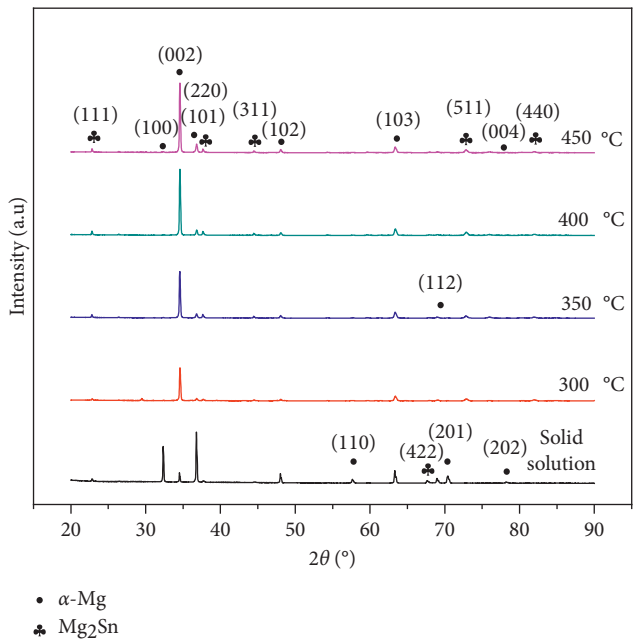

Figure 1: XRD patterns of Mg-6Sn-3Al-Zn alloys without and with rolling at different temperatures.

temperatures are shown in Figure 2. After rolling, (0002) basal plane textures are formed, which is consistent with the XRD result. According to the (0002) basal plane pole figure, the maximum pole density points are distributed in the center of the pole figures. Therefore, it is shown that the basal plane of the alloy is parallel to the rolling direction. The texture intensity increases firstly and then remains unchanged with the increasing of the rolling temperature. When the Mg-6Sn-3Al-Zn alloys are rolled at 300°C, 350°C, 400°C, and 450°C, the texture intensities are 9.45, 12.16, 11.41, and 11.62, respectively.

The OM pictures of the Mg-6Sn-3Al-Zn alloys rolled at different temperature are shown in Figure 3. The black rod-like phase is Mg_2Sn second phase, and the matrix phase is α-Mg phase. The statistical calculations on the average size and volume fraction of Mg_2Sn second phase were performed by Image-Pro Plus 6.0 software, and the variations of them with the rolling temperature are shown in Figure 4. When the rolling temperature was less than or equal to 400°C, the average size and volume fraction of Mg_2Sn phase almost did not change with the rolling temperature increasing. When the alloys were rolled at 300°C, 350°C, and 400°C, the average sizes of Mg_2Sn phase were 18.6 μm, 17.6 μm, and 18.6 μm, respectively, and the volume fractions of Mg_2Sn phase were 3.6%, 3.8%, and 3.8%, respectively. When the rolling temperature reached 450°C, the average size and volume fraction of Mg_2Sn phase increased sharply; for example, their values were 39.3 μm and 9.7%, respectively (shown in Table 1).

EBSD images of the rolled Mg-6Sn-3Al-1Zn alloys with different rolling temperatures are shown in Figure 5. As can be seen from Figure 5, after the alloys were rolled at different temperature, bimodal microstructures were formed, and the grains of the alloy were composed of small grains and large grains.

Misorientation angle distribution diagrams of the rolled Mg-6Sn-3Al-1Zn alloys with different rolling temperatures are shown in Figure 6. As can be seen, a few of {10-12} extension twinning (the angle with parent crystal is 86.1°) and {10-11} contraction twinning (the angle with parent crystal is 56°) exist in deformed alloys.

Twin and high/low-angle boundary distribution diagrams of the rolled Mg-6Sn-3Al-1Zn alloys with different rolling temperatures are shown in Figure 7. As can be seen, the red and blue lines represent the extension twinning boundary and contraction twinning boundary, respectively. The volume fraction of twins is unchanged with the rolling temperature increasing; when the rolling temperatures are 300°C, 350°C, 400°C, and 450°C, the volume fractions of twins are 0.60%, 1.0%, 0.53%, and 0.73%, respectively. Thus, when the rolling temperature is more than or equal to 300°C, the dynamic recrystallization process is completed.

Kernel Average Misorientation (KAM) maps of the rolled Mg-6Sn-3Al-1Zn alloys with different rolling temperatures are shown in Figure 8. As can be seen, the KAM value is almost constant. When the alloys were rolled with 300°C, 350°C, 400°C, and 450°C, the KAM value was 4.98, 4.97, 4.96, and 4.94, indicating that the dynamic recrystallization process is completed as the rolling temperature is more than or equal to 300°C.

The statistical calculations on the average sizes and volume fractions of Mg_2Sn second phase, small grains, and big grains were performed by Image-Pro Plus 6.0 software. And the variations of them with the increasing of the rolling temperature are shown in Figure 4. The average grain size of small grains of the alloy almost does not change with the rolling temperature increasing. And when the alloys are rolled at 300°C, 350°C, 400°C, and 450°C, the average grain sizes of small grains are 3.68 μm, 3.59 μm, 3.66 μm, and 3.72 μm, respectively. When the rolling temperature is less than or equal to 400°C, the average grain size of large grains of alloy decreases with the rolling temperature increasing. For the alloys rolled at 300°C, 350°C, and 400°C, the average grain sizes of large grains are 11.29 μm, 10.05 μm, and 9.24 μm, respectively. When the rolling temperature reaches 450°C, the average grain size of large grains increases to 9.68 μm. When the rolling temperature is less than or equal to 400°C, the volume fraction of small grains of the alloy increases with the rolling temperature increasing. For the alloys rolled at 300°C, 350°C, and 400°C, the volume fractions of small grains are 7.2%, 13.1%, and 18.6%, respectively. When the rolling temperature reaches 450°C, the volume fraction of small grains decreases to 16.4%. The volume fraction of large grains of the alloy decreases with the increasing of the rolling temperature; after the alloy is rolled at 300°C, 350°C, 400°C, and 450°C, the volume fractions of large grains are 89.2%, 83.1%, 77.6%, and 73.9%, respectively, which are shown in Table 1.

The grain size distributions of the alloys rolled at different temperatures which are determined from EBSD images are shown in Figure 9. As can be seen, when the rolling temperature is less than or equal to 400°C, the number of recrystallized grains increases and the average grain size decreases with the rolling temperature increasing.

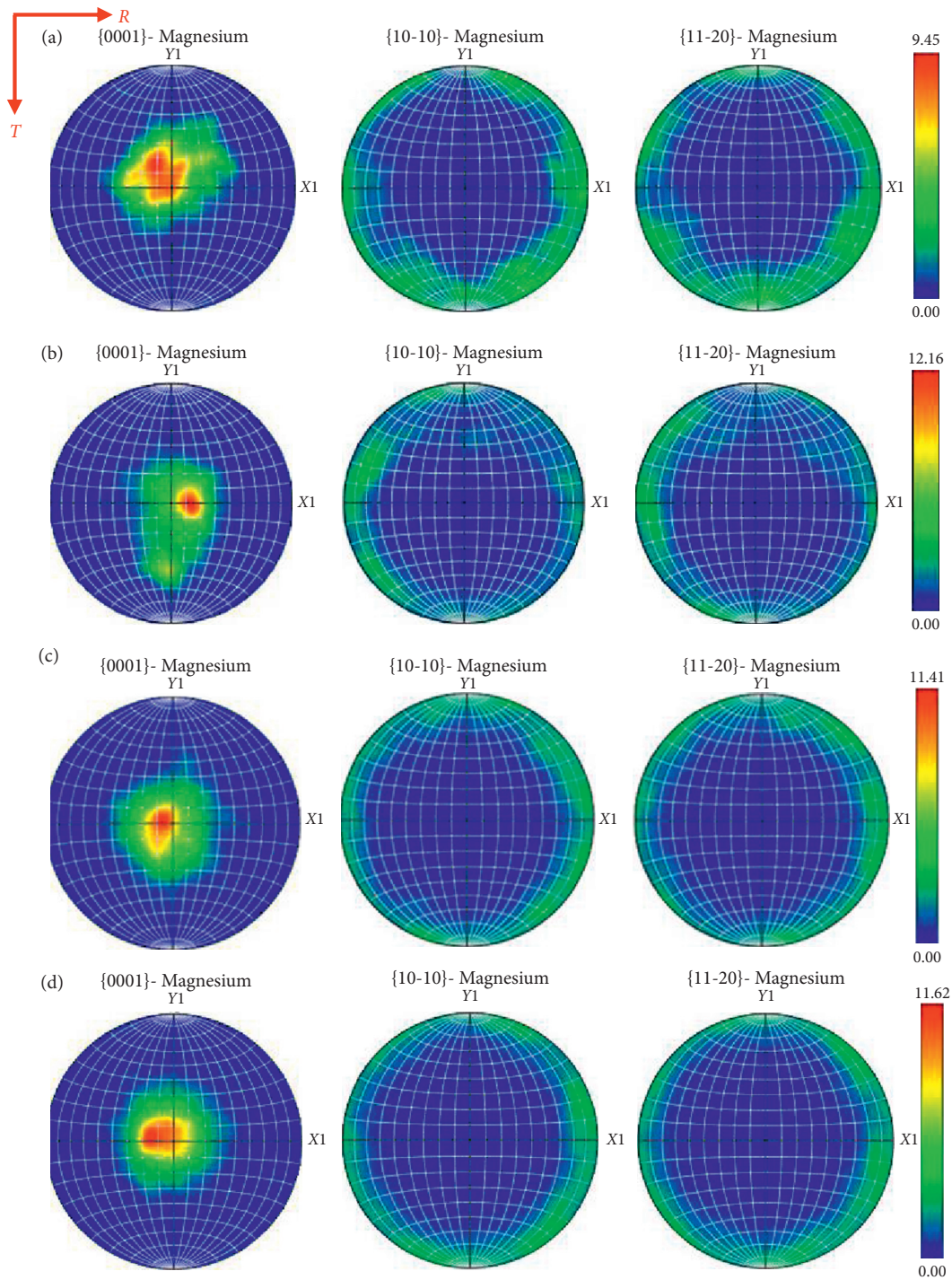

Figure 2: Basal plane (0002), prismatic plane (10-10) and (11-20) pole figures of Mg-6Sn-3Al-Zn alloys rolled at different temperatures: (a) 300°C, (b) 350°C, (c) 400°C, and (d) 450°C.

For the alloy rolled at 300°C, 350°C, and 400°C, the average grain sizes are 7.50 μm, 5.66 μm, and 5.42 μm, respectively. When the rolling temperature reaches 450°C, the average grain size increases to 6.16 μm.

The grain area distributions of the alloys rolled at different temperatures which are determined from EBSD images and the results are shown in Figure 10. When the rolling temperature is more than or equal to 350°C, the bimodal microstructure is clearly formed. With the rolling temperature increasing, the area ranges of big grains firstly decrease and then increase, but the area range of small grains shows a trend of first decreasing and then unchanging. For the alloy rolled at 350°C, the area range of small grains is 0-1250 μm^2, and the area range of big grains is 1450-3550 μm^2. For the alloy rolled at 400°C, the area range of small grains narrows to 0-650 μm^2, while the area ranges of big grains

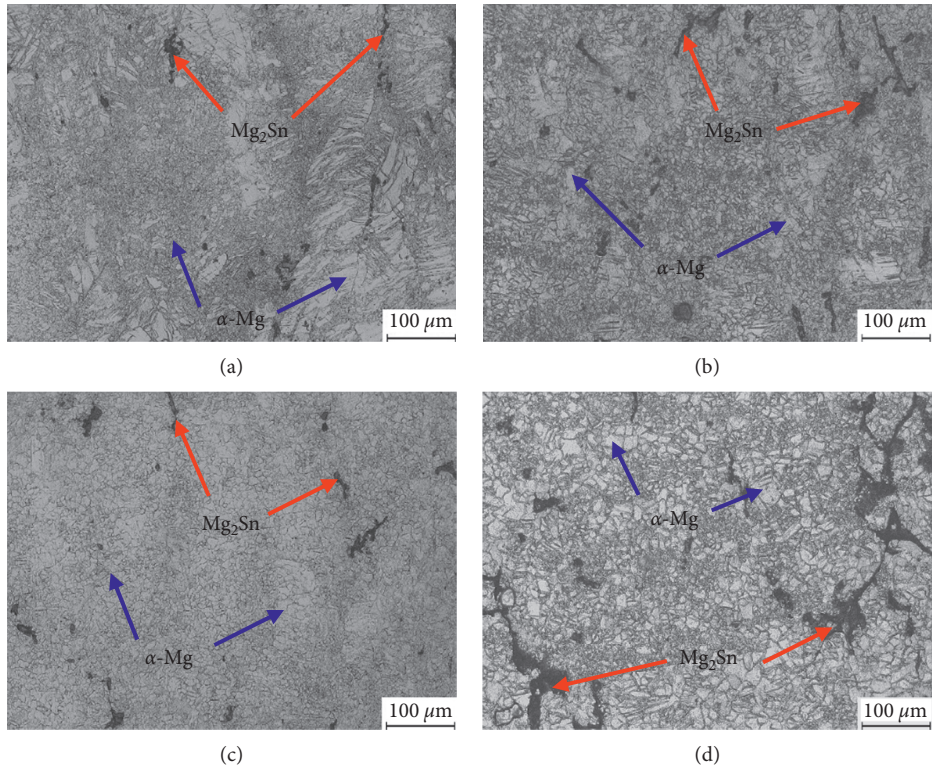

Figure 3: OM pictures of Mg-6Sn-3Al-Zn alloys rolled at different temperatures: (a) 300°C, (b) 350°C, (c) 400°C, and (d) 450°C.

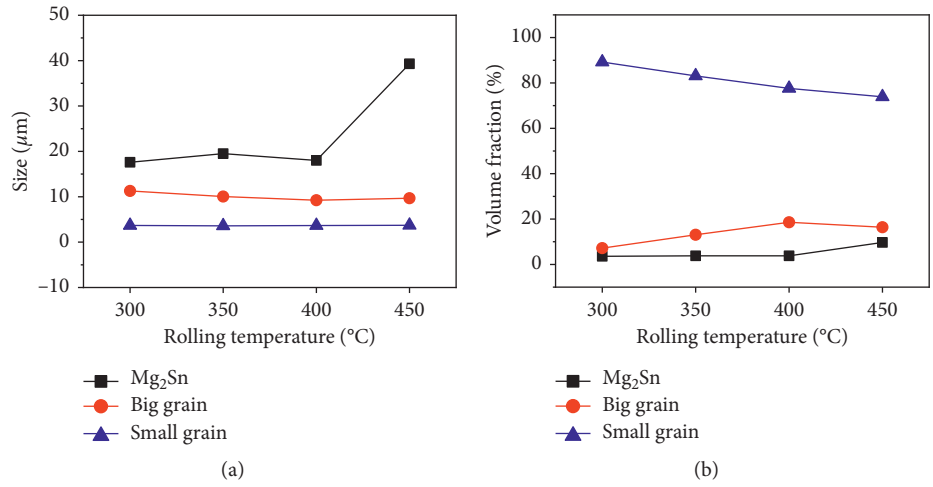

Figure 4: (a) The average grain size of small grains, big grains, and Mg_2Sn phases of the alloys rolled at different temperatures. (b) The volume fraction of small grains, big grains, and Mg_2Sn phases of the alloys rolled at different temperatures.

narrow to 1250-1950 μm^2. For the alloy rolled at 450°C, the area ranges of small grains almost do not change compared to that of the alloy rolled at 400°C, but the volume fraction of small grains decreases, and the area ranges of big grains increase to 1050-3650 μm^2.

The TEM bright field image, selected area electron diffraction (which comes from the blue circle of TEM bright field image and the yellow circle of TEM bright field image), and dark field image (which comes from the white circle of the selected area electron diffraction) of the alloy rolled at 400°C are shown in Figure 11. Dislocation analysis by the invisibility criterion ($g \cdot b = 0$) reveals that the TEM foil contains <a> dislocations and <c+a> dislocations. <c + a> dislocations are visible under both $g = (01\text{-}10)$ and $g = (0002)$, while <a> dislocations are invisible under $g = (0002)$. Hence, these findings agree with the literature (Sabat et al., 2018) [17]. By comparing Figure 11(a) with Figure 11(d), we find that the volume fraction of <a> dislocation is more than that of <c + a> dislocation. Accordingly, these TEM works suggest that the pyramidal plane

Table 1: The average sizes and volume fractions of Mg_2Sn phases, small grains, and big grains of alloys rolled at different temperatures.

Rolling temperature (°C)	The average size (μm)			The volume fraction (%)		
	Small grains	Large grains	Mg_2Sn phases	Small grains	Large grains	Mg_2Sn phases
300	3.68	11.29	18.6	7.2	89.2	3.6
350	3.59	10.05	17.6	13.1	83.1	3.8
400	3.66	9.24	19.5	18.6	77.6	3.8
450	3. 72	9.68	39.3	16.4	73.9	9.7

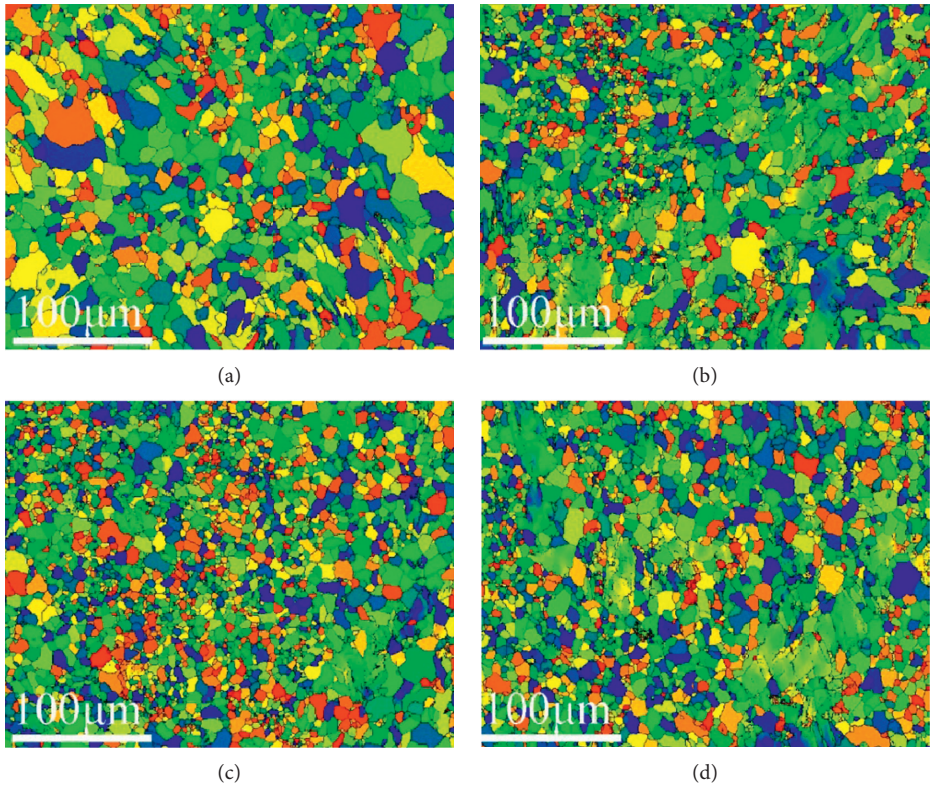

Figure 5: EBSD images of the as-rolled Mg-6Sn-3Al-1Zn alloys at different rolling temperatures: (a) 300°C, (b) 350°C, (c) 400°C, and (d) 450°C.

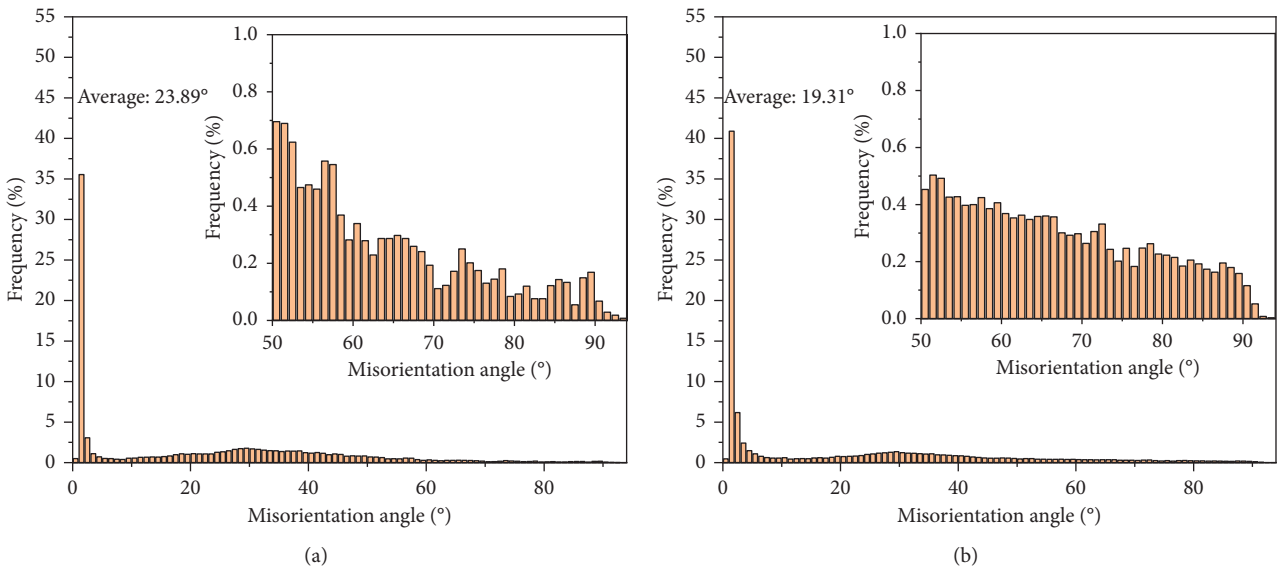

Figure 6: Continued.

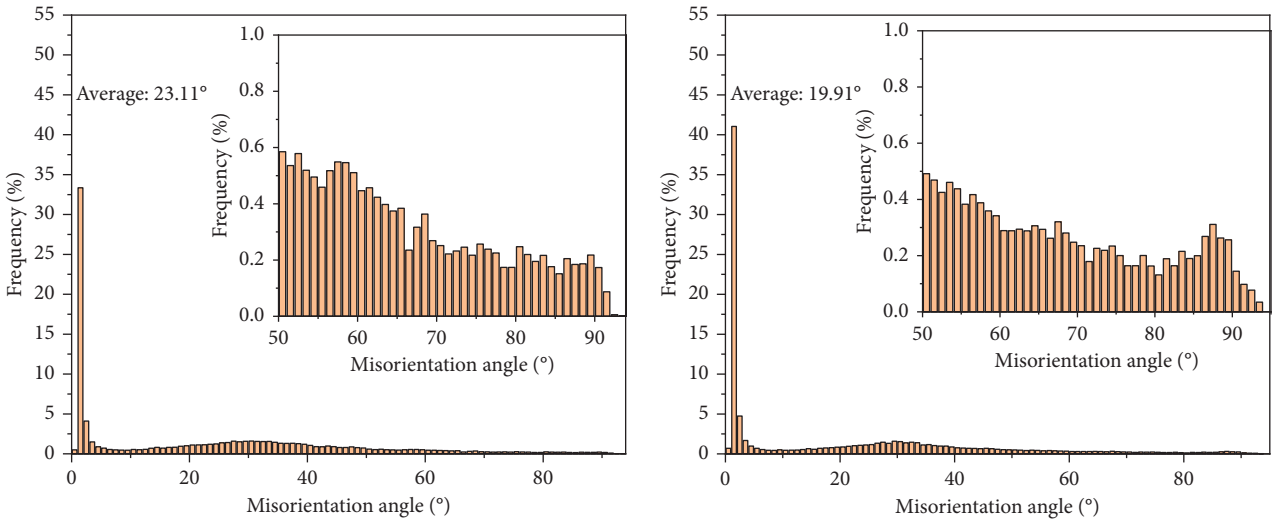

(c) (d)

Figure 6: Misorientation angle distribution diagrams of the as-rolled Mg-6Sn-3Al-1Zn alloys at different rolling temperatures: (a) 300°C, (b) 350°C, (c) 400°C, and (d) 450°C.

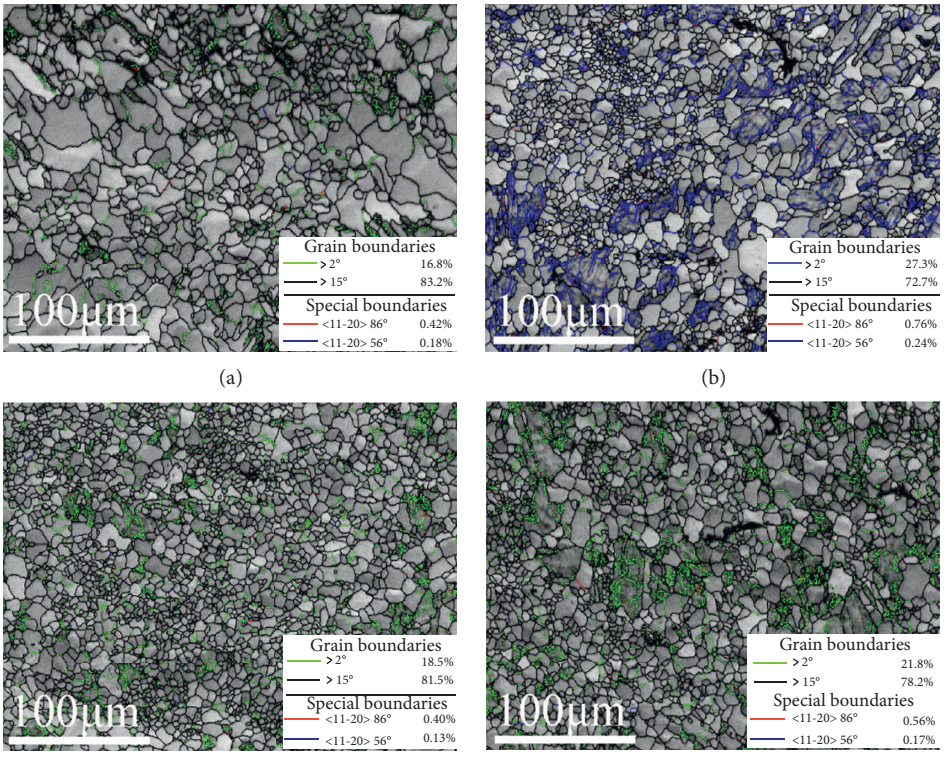

(a) (b)

(c) (d)

Figure 7: Twins and high/low-angle boundary distribution diagrams of the as-rolled Mg-6Sn-3Al-1Zn alloys at different rolling temperatures: (a) 300°C, (b) 350°C, (c) 400°C, and (d) 450°C.

<a> slip is easier to start than the pyramidal plane <$c+a$> slip in the process of rolling, and the SF (stacking fault) energy of pyramidal <a> slip is higher than that of pyramidal <$c+a$> slip, which can be attributed to the more difficult nucleation of <$c+a$> dislocations than that of <a> dislocations. As can be seen from Figure 11(a), the rod-like Mg_2Sn phases, presented in Figure 12, are distributed in the microstructure; the dislocations pile up near the Mg_2Sn phase, indicating that the Mg_2Sn phases could hinder the dislocation motions and then improve alloy strength.

The EDS (Energy Dispersive Spectrometer) mappings of the alloy rolled at 400°C are shown in Figure 12. As can be

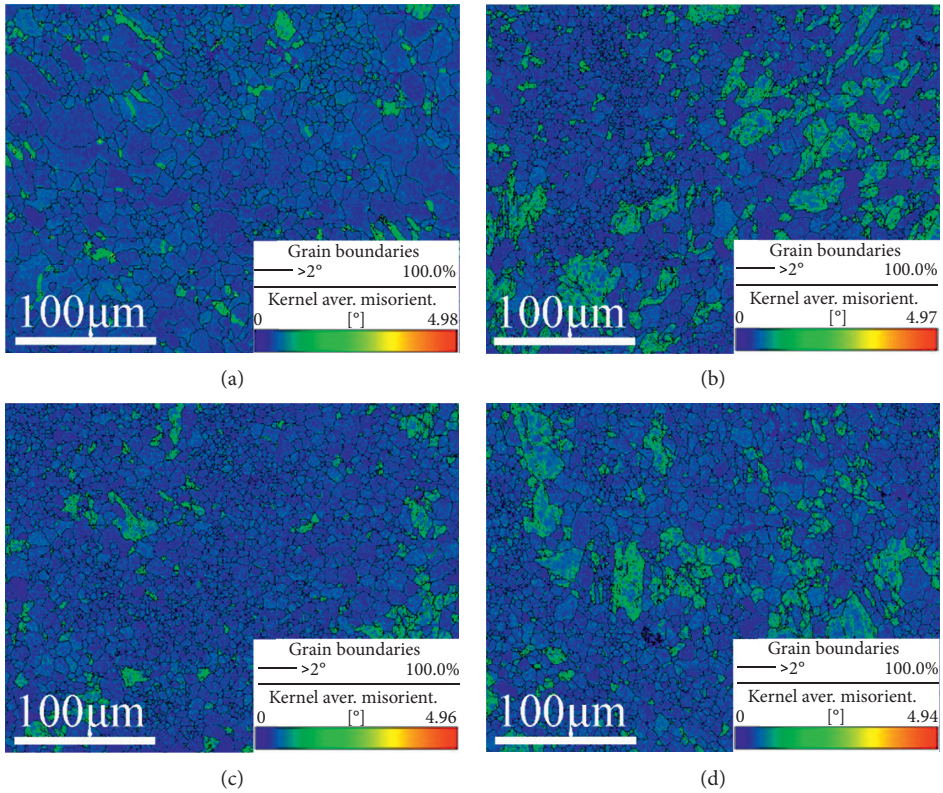

Figure 8: Kernel Average Misorientation maps of the as-rolled Mg-6Sn-3Al-1Zn alloys at different rolling temperatures: (a) 300°C, (b) 350°C, (c) 400°C, and (d) 450°C.

seen from Figure 12(a), a few of rod-like phases are distributed in the TEM bright field image. We select a rectangular region for EDS mapping. As can be seen from Figure 12(e), the Sn element is rich and shows rod-like pattern, indicating that the rod-like phases in TEM bright field image are Mg_2Sn phase, and this result is consistent with XRD result. Moreover, as can be seen, the Mg, Al, and Zn elements are distributed uniformly in the microstructure.

The tensile stress-strain curves of the alloys rolled at different temperatures, the changes of tensile mechanical properties, and Vickers hardness of the alloys with rolling temperature are shown in Figure 13 and summarized in Table 2. When the rolling temperature is less than or equal to 400°C, yield strength of the alloy increases from 267.8 MPa for the alloy rolled at 300°C to 289.5 MPa for the alloy rolled at 400°C. When the rolling temperature reaches 450°C, yield strength of the alloy decreases to 235.3 MPa. When the alloy is rolled at 350°C, the tensile strength of the alloy almost does not change compared to the alloy rolled at 300°C. For the alloy rolled at 400°C, its tensile strength increases to 361.1 MPa. When the rolling temperature reaches 450°C, tensile strength of the alloy decreases to 318.9 MPa. The elongation of the alloy increases with the rolling temperature increasing. For the alloys rolled at 300°C, 350°C, 400°C, and 450°C, their elongations are 11.2%, 19.3%, 20.5%, and 21.1%, respectively. The Vickers hardness of the alloy decreases with the rolling temperature increasing. For the alloys rolled at 300°C, 350°C, 400°C, and 450°C, their hardness values are 80.9 HV, 79.1 HV, 76.3 HV, and 66.3 HV, respectively. Importantly, for the alloy rolled at 400°C, the tensile strength and plasticity reach the best combination.

4. Discussion

4.1. Effect of Rolling Temperature on Bimodal Microstructure. When the rolling temperature is less than or equal to 400°C, with the rolling temperature increasing, the average grain size of large grains of alloy decreases, and the volume fraction of small grains of alloy increases. It is because the rolling temperature is higher than the recrystallization temperature. High rolling temperature and large rolling deformation sufficiently promote the recrystallization process of alloys. Hence, the higher the rolling temperature, the smaller the grains formed after rolling. When the rolling temperature reaches 450°C, the average grain size of large grains increases, and the volume fraction of small grains decreases. This is because the rolling temperature is too high, resulting in grain size growth.

4.2. Effect of Rolling Temperature on Mg_2Sn Phase. Low rolling temperature will separate out Mg_2Sn phase from matrix. However, the rolling period is very short. Therefore, when the rolling temperature is less than or equal to 400°C, the volume fraction of Mg_2Sn phase almost does not change with the rolling temperature increasing. When the rolling temperature reaches 450°C, the average size and volume fraction of Mg_2Sn phase increase sharply. This is owing to

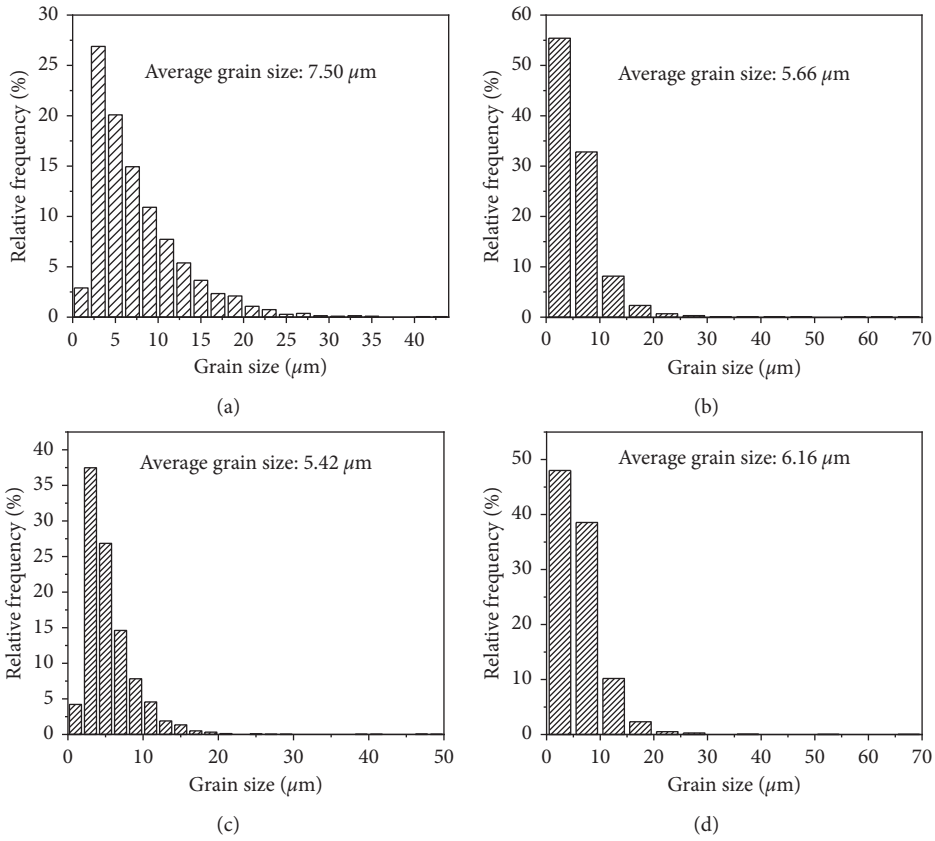

Figure 9: Grain size distributions of the alloys rolled at different temperatures which were determined from EBSD images: (a) 300°C, (b) 350°C, (c) 400°C, (d) 450°C.

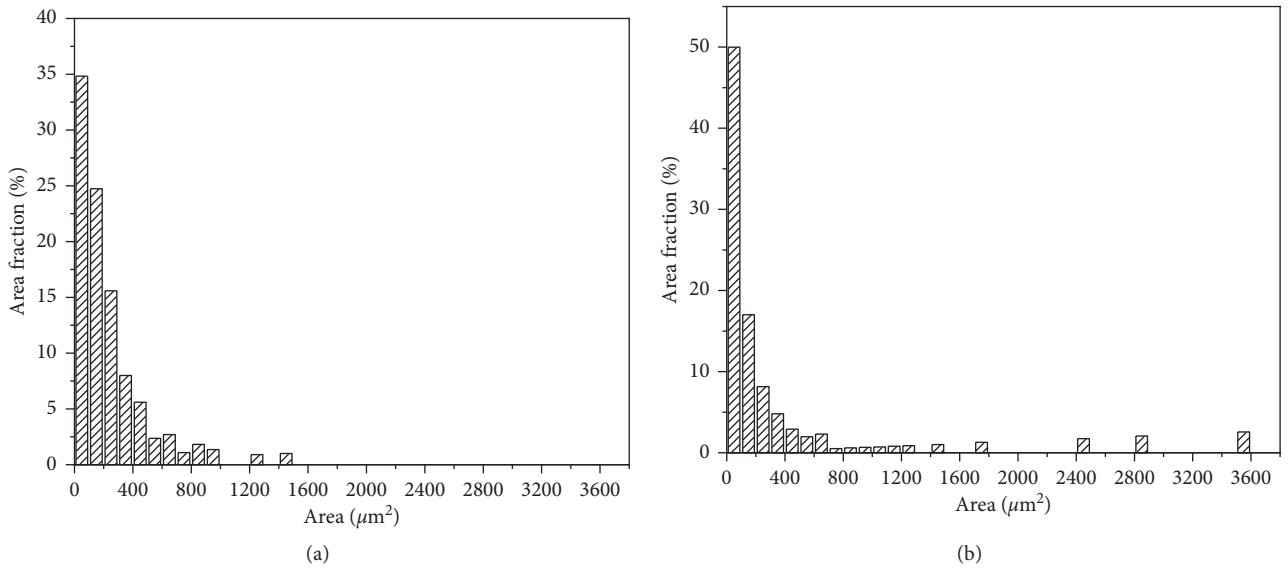

Figure 10: Continued.

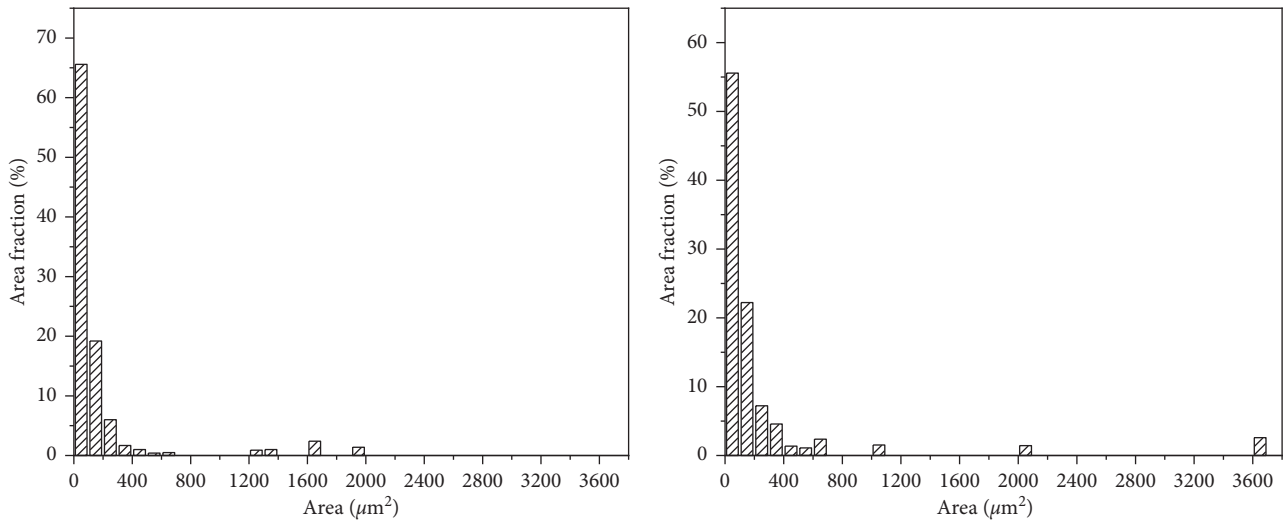

Figure 10: Grain area distributions of the alloys rolled at different temperatures which were determined from EBSD images: (a) 300°C, (b) 350°C, (c) 400°C, and (d) 450°C.

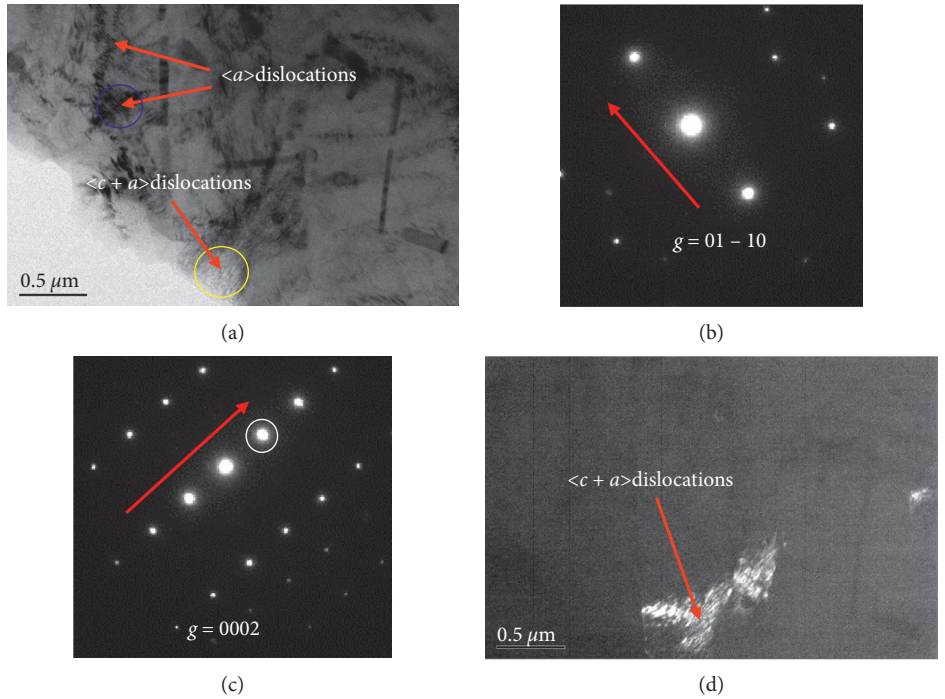

Figure 11: The TEM bright field image (a), selected area electron diffraction (b, c), and the TEM dark field image (d) of the alloy rolled at 400°C. $<c+a>$ dislocations were identified in a grain based on the invisibility criterion; $<a>$ dislocations were also found in their vicinity. Two-beam dark-field images were taken along the [2-1-10] zone axis under $g = (01\text{-}10)$ and $g = (0002)$, respectively.

the phenomenon that high rolling temperature will lead to Mg_2Sn phase separated out from the solid solution. However, the average size of Mg_2Sn phase almost does not change with the rolling temperature increasing. It is because the Mg_2Sn phase belongs to the hard brittle phase, and in this work, the amount of rolling deformation is 60%; the force for breaking resistance of Mg_2Sn phase is the same.

4.3. Effect of Rolling Temperature on Mechanical Properties. When the rolling temperature is less than or equal to 400°C, with the rolling temperature increasing, the yield strength of the alloy increases, which can be attributed to the grain size of large grains decreasing and the volume fraction increasing; then, the fine grain strengthening effect is obvious. When the rolling temperature reaches 450°C, the yield strength of the alloy

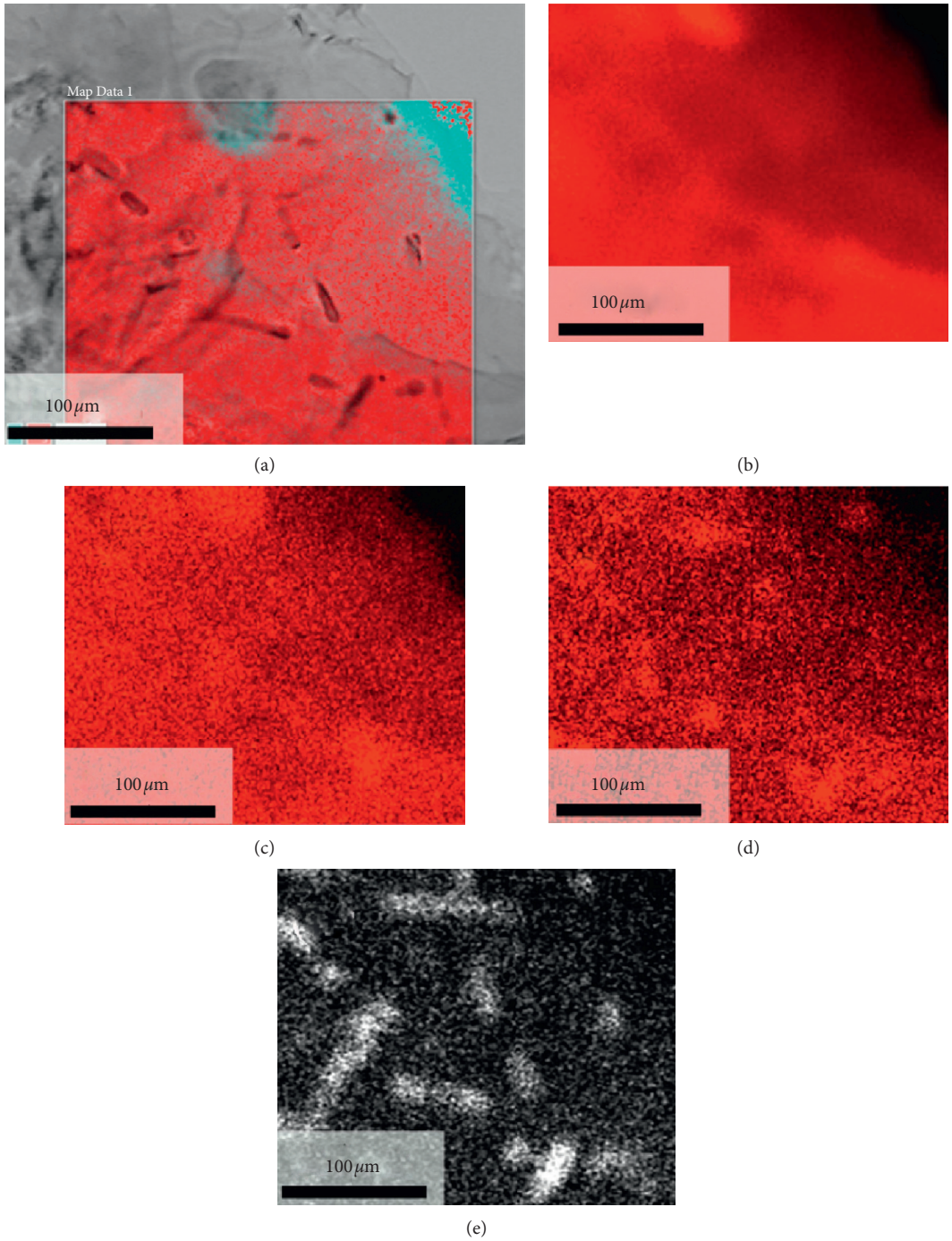

FIGURE 12: The EDS mapping of the alloy with a rolling temperature of 400°C. (a) Selected region from TEM bright field image, (b) Mg element, (c) Al element, (d) Zn element, and (e) Sn element.

decreases, because the grain size clearly increases. Otherwise, although the volume fraction of Mg_2Sn phase increases, the average size of Mg_2Sn phase is large; thus, the dispersion strengthening effect is weakened.

When the alloy was rolled at 350°C, a bimodal microstructure was clearly formed. This leads to the elongation increasing sharply. Otherwise, due to the high rolling temperature, the pyramidal plane $<a>$ slip and $<c+a>$ slip started in the process of rolling. The higher the rolling temperature of alloy, the easier to start the dislocation motion. This showed that the elongation of the alloy increases with the rolling temperature increasing. When the

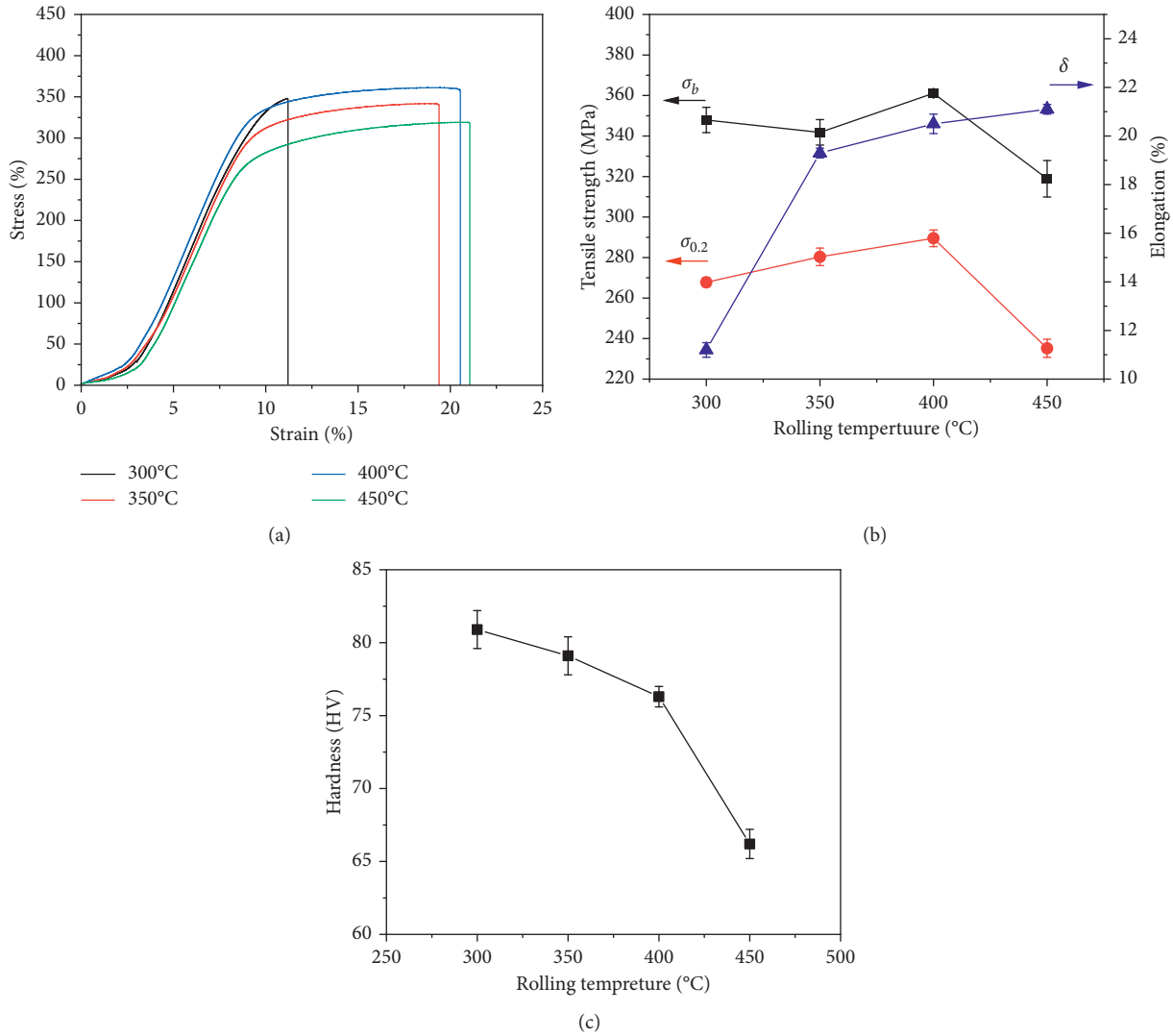

Figure 13: The tensile stress-strain curves of the alloys rolled at different temperatures (a), the changes of tensile mechanical properties (b), and Vickers hardness (c) of the alloys with rolling temperatures.

Table 2: Mechanical properties of alloy rolled at different temperatures.

Rolling temperature (°C)	Tensile strength (MPa) (mean ± SD)	Yield strength (MPa) (mean ± SD)	Elongation (%) (mean ± SD)	Vickers hardness (HV) (mean ± SD)
300	347.9 ± 6.2	267.8 ± 2.3	11.2 ± 0.3	80.9 ± 1.3
350	341.8 ± 6.3	277.3 ± 4.3	19.3 ± 0.2	79.1 ± 1.3
400	361.1 ± 0.6	289.5 ± 4.1	20.5 ± 0.4	76.3 ± 0.7
450	318.9 ± 9.0	235.3 ± 4.5	21.1 ± 0.2	66.3 ± 1.0

alloy was rolled at 450°C, the area ranges of large grains increased, which led to the elongation further increasing.

5. Conclusions

The Mg-6Sn-3Al-1Zn alloys are composed of Mg_2Sn phase and α-Mg matrix phase. When the rolling temperature was less than or equal to 400°C, with the rolling temperature increasing, the average size and volume fraction of Mg_2Sn second phase and the average grain size of small grains remain unchanged. Due to the dynamic recrystallization during the rolling process, the average grain size of large grains decreased, and the volume fraction of small grains increased, which led to the yield strength of the alloy increasing. When the rolling temperature reached 450°C, due to the high rolling temperature, the average grain size of large grains increased, the volume fraction of small grains decreased, and the average size and volume fraction of Mg_2Sn phase and the yield strength of the alloy decreased. With the rolling temperature increasing, the elongation increased, but the hardness change had an opposite trend. When the rolling

temperature reached 400°C, the average size of small grains, large grains, and Mg_2Sn phase was 3.66 μm, 9.24 μm, and 19.5 μm, and the volume fraction of small grains, large grains, and Mg_2Sn phase was 18.6%, 77.6%, and 3.8%, respectively. Accordingly, the tensile properties reached the optimum; i.e., the tensile strength, yield strength, elongation, and Vickers hardness were 361.1 MPa, 289.5 MPa, 20.5%, and 76.3 HV, respectively.

Data Availability

The data used to support the findings of this study are available from the corresponding author upon request.

Conflicts of Interest

The authors declare no conflicts of interest.

Authors' Contributions

F. W. contributed to conceptualization and writing—original draft preparation; B. S. contributed to methodology; J. W. contributed to investigation; P. L. and B. S. contributed to writing—review and editing. All authors have read and agreed on the published version of the manuscript.

Acknowledgments

This research was funded by Qing Hai Provincial Natural Science Foundation (Grant No. 2020-ZJ-707).

References

[1] S. Sandlöbes, M. Friák, S. Korte-Kerzel, Z. Pei, J. Neugebauer, and D. A. Raabe, "Rare-earth free magnesium alloy with improved intrinsic ductility," *Scientific Reports*, vol. 7, no. 1, pp. 1–8, 2017.

[2] T. T. T. Trang, J. H. Zhang, J. H. Kim et al., "Designing a magnesium alloy with high strength and high formability," *Nature Communications*, vol. 9, no. 1, pp. 1–6, 2018.

[3] K. Hamad and Y. G. Ko, "A cross-shear deformation for optimizing the strength and ductility of AZ31 magnesium alloys," *Scientific Reports*, vol. 6, no. 1, pp. 1–8, 2016.

[4] Z. Wu, R. Ahmad, B. Yin, S. Sandlöbes, and W. A. Curtin, "Mechanistic origin and prediction of enhanced ductility in magnesium alloys," *Science*, vol. 359, no. 6374, pp. 447–452, 2018.

[5] S. Tang, T. Z. Xin, W. Q. Xu et al., "Precipitation strengthening in an ultralight magnesium alloy," *Nature Communications*, vol. 10, no. 1, pp. 1–8, 2019.

[6] H. Pan, G. Qin, Y. Huang et al., "Development of low-alloyed and rare-earth-free magnesium alloys having ultra-high strength," *Acta Materialia*, vol. 149, pp. 350–363, 2018.

[7] W. J. Joost and P. E. Krajewski, "Towards magnesium alloys for high-volume automotive applications," *Scripta Materialia*, vol. 128, pp. 107–112, 2017.

[8] L. Wang, E. Mostaed, X. Cao et al., "Effects of texture and grain size on mechanical properties of AZ80 magnesium alloys at lower temperatures," *Materials & Design*, vol. 89, pp. 1–8, 2016.

[9] M. Zha, X. H. Zhang, H. Zhang et al., "Achieving bimodal microstructure and enhanced tensile properties of Mg-9Al-1Zn alloy by tailoring deformation temperature during hard plate rolling (HPR)," *Journal of Alloys and Compounds*, vol. 765, pp. 1228–1236, 2018.

[10] H.-M. Zhang, X.-M. Cheng, M. Zha et al., "A superplastic bimodal grain-structured Mg-9Al-1Zn alloy processed by short-process hard-plate rolling," *Materialia*, vol. 8, pp. 100443–100449, 2019.

[11] M. Zha, Y. Li, R. H. Mathiesen, R. Bjørge, and H. J. Roven, "Achieve high ductility and strength in an Al-Mg alloy by severe plastic deformation combined with inter-pass annealing," *Materials Science and Engineering: A*, vol. 598, pp. 141–146, 2014.

[12] M. Zha, Y. Li, R. H. Mathiesen, R. Bjørge, and H. J. Roven, "High ductility bulk nanostructured Al-Mg binary alloy processed by equal channel angular pressing and inter-pass annealing," *Scripta Materialia*, vol. 105, pp. 22–25, 2015.

[13] M. Zha, Y. Li, R. H. Mathiesen, R. Bjørge, and H. J. Roven, "Microstructure evolution and mechanical behavior of a binary Al-7Mg alloy processed by equal-channel angular pressing," *Acta Materialia*, vol. 84, pp. 42–54, 2015.

[14] B. Wang, F. Pan, X. Chen, W. Guo, and J. Mao, "Microstructure and mechanical properties of as-extruded and as-aged Mg-Zn-Al-Sn alloys," *Materials Science and Engineering: A*, vol. 656, pp. 165–173, 2016.

[15] S. H. Park, S.-H. Kim, H. S. Kim, J. Yoon, and B. S. You, "High-speed indirect extrusion of Mg-Sn-Al-Zn alloy and its influence on microstructure and mechanical properties," *Journal of Alloys and Compounds*, vol. 667, pp. 170–177, 2016.

[16] W. Cheng, L. Tian, H. Wang, L. Bian, and H. Yu, "Improved tensile properties of an equal channel angular pressed (ECAPed) Mg-8Sn-6Zn-2Al alloy by prior aging treatment," *Materials Science and Engineering: A*, vol. 687, pp. 148–154, 2017.

[17] R. K. Sabat, A. P. Brahme, R. K. Mishra et al., "Ductility enhancement in Mg-0.2% Ce alloys," *Acta Mater*, vol. 161, pp. 246–257, 2018.